

Cite this: *Chem. Sci.*, 2016, **7**, 3147Received 26th October 2015  
Accepted 20th January 2016DOI: 10.1039/c5sc04060d  
[www.rsc.org/chemicalscience](http://www.rsc.org/chemicalscience)

## Introduction

The ability to transform a carbon–hydrogen bond to a carbon–heteroatom bond is highly important owing to its involvement in late-stage functionalization of complex natural products, pharmaceuticals and agrochemicals.<sup>1</sup> An effective strategy in this domain is yet to achieve its full potential due to the inherent problem of the selectivity and reactivity of the carbon–hydrogen bond.<sup>2</sup> Although the concept of directing-group (DG) assistance resolves the issue of the selective functionalization of the proximal C–H bond,<sup>3</sup> the distal *meta*-C–H bond is difficult to activate.<sup>2b,4</sup> Hence the intrinsic electronic bias of the substituted core has been utilized to promote *meta*-C–H functionalization.<sup>5</sup> In order to reach the remote *meta*-C–H bond the idea of a traceless directing group, transient mediators and the concept of H-bonding have been utilized.<sup>6</sup> However, regardless of the functionalization, template assisted direct *meta*-C–H bond activation requires the involvement of a large strained metalacycle intermediate. Therefore success relies on the perfect design of the directing group (DG) linkage, the coordinating site and the choice of metals. In 2012, pioneering work by Yu and co-workers demonstrated the feasibility of the hypothesis using a U-shaped template with a tethered –CN directing group.<sup>7</sup> The concept was explored in various arylamine, benzylamine, cinnamic acid, phenol, benzyl alcohol and phenyl acetic acid scaffolds by the same group to elucidate the directing group assisted C–C and C–O bond formations *via* olefination, arylation, alkylation and acetoxylation reactions.<sup>7,8</sup> Furthermore, the concept of optimal coordination by a –CN directing group has

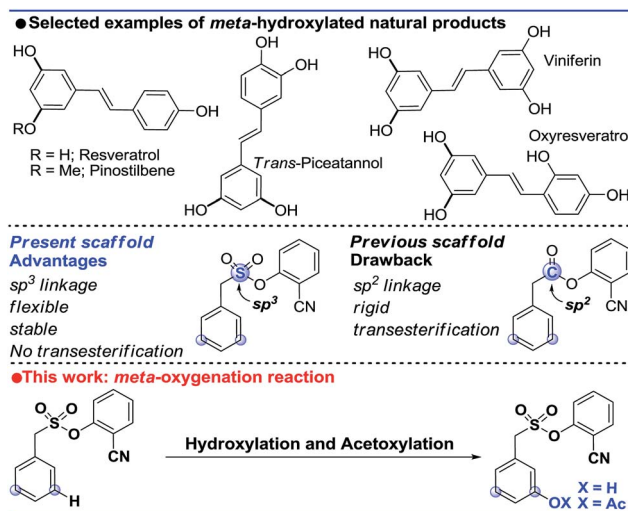
## Directing group assisted *meta*-hydroxylation by C–H activation†

Arun Maji, Bangaru Bhaskararao, Santanu Singha, Raghavan B. Sunoj\* and Debabrata Maiti\*

*meta*-Hydroxylated cores are ubiquitous in natural products. Herein, we disclose the first template assisted *meta*-hydroxylation reaction. Experimental and *in silico* studies helped us to gain valuable mechanistic insights, including the role of the hexafluoroisopropanol (HFIP) solvent, during C–H hydroxylation. The reactive intermediates, prior to the C–H activation, have been detected by spectroscopic techniques. Additionally, the C–O bond formation has been extended to *meta*-acetoxylation. The preparation of a phase II quinone reductase activity inducer and a resveratrol precursor illustrated the synthetic significance of the present strategy.

been extended by the Tan group, our group and recently by the Li group towards benzylsilyl, benzylsulphonyl, phenyl acetic acid and phenylethyl amine derivatives.<sup>9</sup> Despite significant progress in template assisted *meta* selective C–C bond formation, the generation of a C–X (heteroatom) bond at the *meta* position is still in its infancy.

Following our initial report on the *meta*-olefination of the phenylacetic acid core (Scheme 1),<sup>9b</sup> an arylmethane sulphonyl moiety was noted to mitigate the *trans*-esterification issues noted in earlier work.<sup>9c</sup> Moreover *meta*-C–O bond formation with phenylacetic acid was found to be problematic. Therefore, we planned a *meta*-hydroxylation reaction with an arylmethane sulphonyl core as the model substrate. Despite the successful acetoxylation of arylamine,<sup>8c</sup> benzylamine and indoline



Scheme 1 Overview of the present work.

Department of Chemistry, IIT Bombay, Powai, Mumbai-400076, India. E-mail: [dmaiti@chem.iitb.ac.in](mailto:dmaiti@chem.iitb.ac.in); [sunoj@chem.iitb.ac.in](mailto:sunoj@chem.iitb.ac.in)

† Electronic supplementary information (ESI) available. CCDC 1417521–1417523. For ESI and crystallographic data in CIF or other electronic format see DOI: 10.1039/c5sc04060d

scaffolds<sup>8d</sup> by Yu and coworkers, a single-step *meta*-hydroxylation protocol is yet to be reported.

## Results and discussion

Our initial attempts at direct hydroxylation failed owing to the intolerance of the cyano directing group towards strong oxidizing conditions (Table 1). Hence we envisioned installing an oxygenating group under mild oxidizing conditions followed by its *in situ* hydrolysis.<sup>10</sup> With PhI(TFA)<sub>2</sub> (4 equiv.) as the hydroxylating agent,<sup>11</sup> and *N*-formyl-glycine (For-Gly-OH, 25 mol%) as the ligand for Pd(OAc)<sub>2</sub> (10 mol%) in HFIP solvent, the desired *meta*-hydroxylated compound was obtained in a 78% (isolated, 74%) yield and with excellent selectivity (32 : 1).

Using the optimized conditions, the scope of the reaction was explored (Table 2). Electron rich alkyl substituted arenes were hydroxylated with good yield and excellent selectivity (**1b**, **1c** and **1g**). Steric crowding in the close vicinity of the *meta*-C–H bond was found to affect the formation of the palladated intermediate. Moving from –Me (**1b**) to –iPr (**1c**) as the *para* substituent, the yield declined from 77% to 63%. In disubstituted systems, replacing chloro (**1h**) with bromo (**1i**) enhanced the selectivity towards the less hindered *meta*-C–H bond (**1h**, 65% and **1i**, 63%). Groups such as –OPh, –OCF<sub>3</sub>, and –OMe were also tolerated.

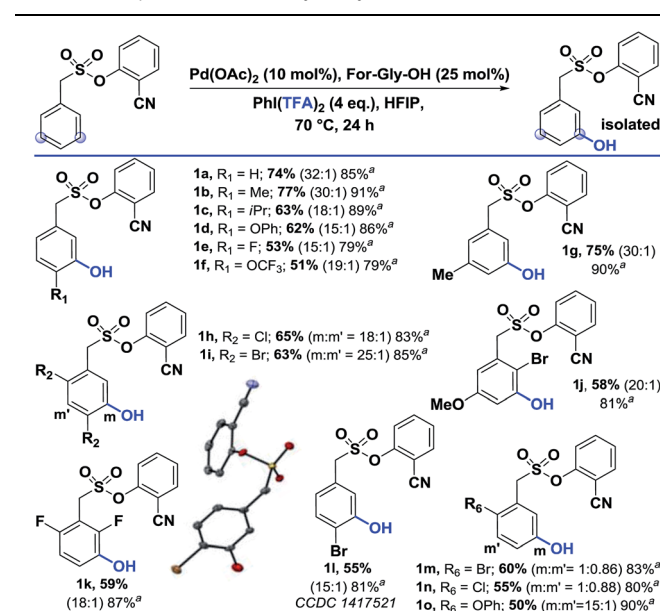
Interestingly, changing the acetoxylation agent from PhI(TFA)<sub>2</sub> to PhI(OAc)<sub>2</sub> led to the formation of the *meta*-acetoxylated compound as the sole product. Due to the importance of the *meta*-acetoxylated compounds, the protocol was optimized and the scope was explored. For *meta*-acetoxylation, *N*-*tert*-butyloxycarbonyl-alanine (Boc-Ala-OH) was found to be the best ligand for palladium. A similar reactivity trend to that of hydroxylation was observed for acetoxylation (Table 3).

Table 1 Different hydroxylation approaches<sup>12,c</sup>

| Catalyst <sup>a</sup>                     | –OH source  | Yield |
|---|---|-------|
| 1 PdCl <sub>2</sub> /Pd(OAc) <sub>2</sub> | TBHP (4 eq.)  | 0     |
| 2 PdCl <sub>2</sub>                       | H <sub>2</sub> O <sub>2</sub> (4 eq.)   | 0     |
| 3 PdCl <sub>2</sub>                       | NHPI (2 eq.)  | 0     |
| 4 Cu(OAc) <sub>2</sub>                    | (PhCO) <sub>2</sub> O (2 eq.), HFIP (1 mL)  | 0     |
| 5 PdCl <sub>2</sub> /Pd(OAc) <sub>2</sub> | TEMPO (2 eq.)   | 0     |
| 6 Cu(OAc) <sub>2</sub>                    | TBAI (2 eq.), Ag <sub>2</sub> CO <sub>3</sub> (2 eq.)                               | 0     |
| 7 PdCl <sub>2</sub>                       | K <sub>2</sub> S <sub>2</sub> O <sub>8</sub> (2 eq.), CF <sub>3</sub> COOH (0.5 mL) | 0     |
| 8 Pd(OAc) <sub>2</sub>                    | Na <sub>2</sub> S <sub>2</sub> O <sub>8</sub> (2 eq.); dioxane (1 mL)               | 0     |
| 9 <sup>b</sup> Pd(OAc) <sub>2</sub>       | PhI(TFA) <sub>2</sub> (4 eq.), (CF <sub>3</sub> CO) <sub>2</sub> O                  | 11    |
| 10 Pd(OAc) <sub>2</sub>                   | PhI(TFA) <sub>2</sub> (4 eq.), HFIP (1 mL)  | 78    |

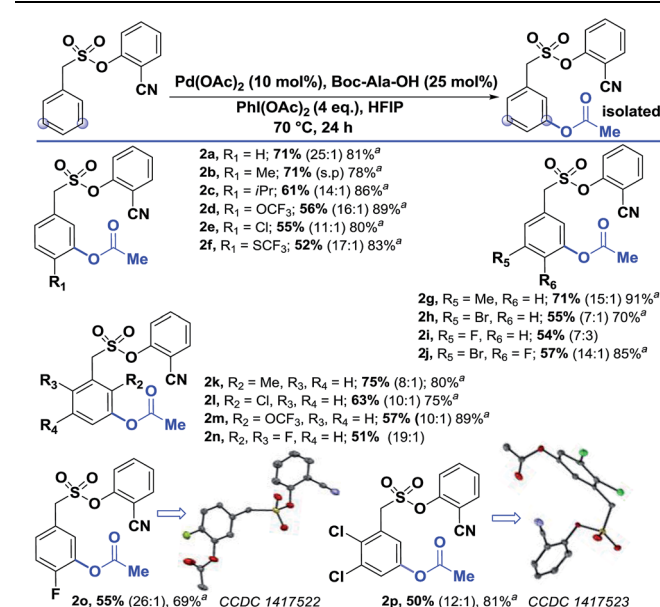
<sup>a</sup> Catalyst loading 10 mol%. <sup>b</sup> 0.5 mL of (CF<sub>3</sub>CO)<sub>2</sub>O added. <sup>c</sup> 70 °C was maintained for all the reactions; all the reactions were performed on a 0.2 mmol scale.

Table 2 Scope of the *meta*-hydroxylation<sup>13,b</sup>



<sup>a</sup> These yields are based on the recovered starting material. <sup>b</sup> All the reactions were performed on a 0.2 mmol scale with Pd(OAc)<sub>2</sub> (0.1 equiv.), For-Gly-OH (0.25 equiv.), PhI(TFA)<sub>2</sub> (4 equiv.), and HFIP (1 mL). All the selectivity ratios (*meta*:others) were obtained from the crude reaction mixtures using 1,3,5-trimethoxybenzene as a reference. (m:m').

Table 3 Scope of the *meta*-acetoxylation<sup>13,b</sup>



<sup>a</sup> These yields are based on the recovered starting material. <sup>b</sup> All the reactions were performed on a 0.2 mmol scale with Pd(OAc)<sub>2</sub> (0.1 equiv.), Boc-Ala-OH (0.25 equiv.), PhI(OAc)<sub>2</sub> (4 equiv.), and HFIP (1 mL) all the selectivity ratios (*meta*:others) were obtained from the crude reaction mixtures using 1,3,5-trimethoxybenzene as a reference.



Notably, in the standard one-pot approach no dihydroxylation or diacetoxylation products were detected. Although hydroxyl groups are known to direct the metal to the proximal C–H bond, no such difunctionalization was observed under the present reaction conditions.

Arguably, the difference in ligand environment, competitive coordination with the –CN and hindered deprotonation of the phenol under the mildly acidic conditions of the reaction mixture reduces the scope for undesired functionalization of the product.<sup>14</sup>

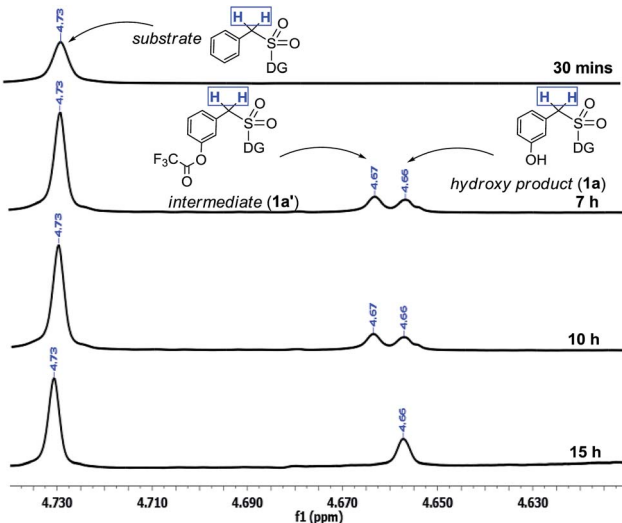
### Intermediate detection

The interesting switch from hydroxylation to acetoxylation upon changing the –R group on  $\text{PhI(OOCR)}_2$  from  $-\text{CF}_3$  to  $-\text{CH}_3$  can be justified by the reduced electrophilicity of the ester carbonyl in the acetate as compared to that in the trifluoroacetate, which disfavors hydrolysis and thus the product remains acetoxylated. This observation is additionally supported by a computational study (*vide infra*).

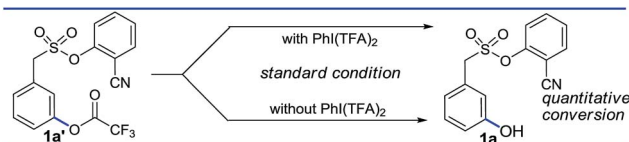
Moreover the quantitative conversion of an independently synthesized *meta*-trifluoroacetoxylated substrate to the *meta*-hydroxy compound under the standard reaction conditions (Scheme 3) supported our initial hypothesis for the hydroxylation strategy.<sup>12</sup> Furthermore, the intermediacy of the trifluoroacetoxylated compound as a hydroxyl precursor has been intercepted through NMR study (Scheme 2).

### Mechanistic study

During the optimization of the reaction conditions, HFIP and the N-protected aminocarboxylic acid ligand were found to be indispensable. To gain better insights into the mechanistic complexity, the reaction was monitored by NMR. Interestingly, in the presence of stoichiometric  $\text{Pd(OAc)}_2$  and the ligand, the addition of the substrate intensified the acetic acid ( $-\text{CH}_3$ ) peak,



Scheme 2 Reaction profile of *meta*-hydroxylation. <sup>a</sup>Reactions were performed with 1.5 equiv. of  $\text{PhI(TFA)}_2$ .



Scheme 3 Generation of hydroxyl compounds via hydrolysis.

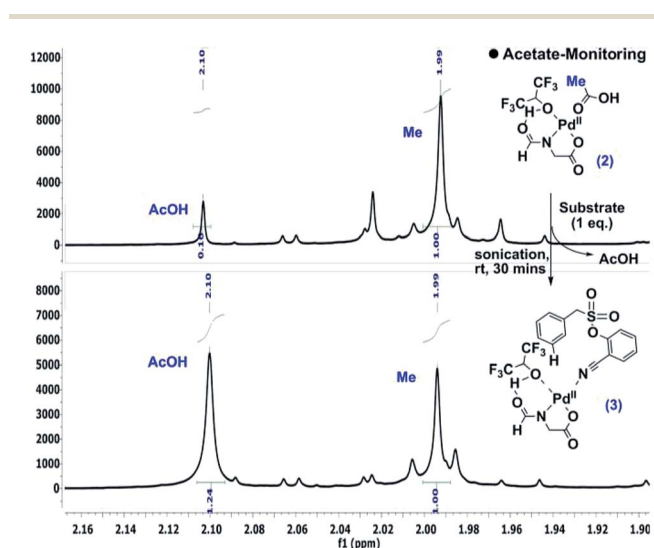
which indicates the release of acetic acid from the metal complex (Scheme 4).<sup>12</sup>

Upon standing, the splitting pattern of the target aromatic ring was found to be disturbed (Scheme 5). Control experiments revealed that the palladium is essential for such splitting variation in the aromatic region. Such an observation can be visualized as the weak interaction between the substrate and palladium, likely the CN-anchored one, which eventually leads to the C–H activation.

The interaction between the palladium and the substrate could also be observed from the variation in the C–N bond stretching frequency. Upon addition of stoichiometric  $\text{Pd(OAc)}_2$  to the substrate, the –CN peak position shifted from  $2237\text{ cm}^{-1}$  to  $2247\text{ cm}^{-1}$ , which further shifted to  $2250\text{ cm}^{-1}$  upon addition of a stoichiometric amount of ligand. Moreover, solvated (MeOH and MeCN) For-Gly-OH ligated palladium species could be identified through mass spectroscopy.

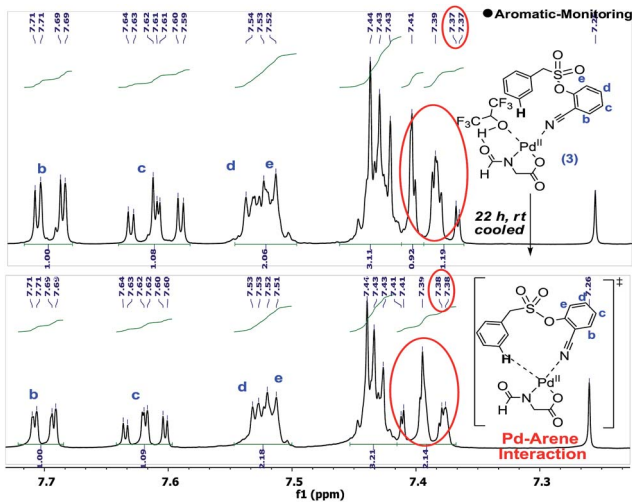
All of these observations pointed towards a facile interaction of the substrate, ligand and HFIP with the palladium centre under ambient temperature. Despite these interactions, none of the desired product was formed at room temperature. This could be indicative of the fact that the C–H activation and the ensuing steps are more energy demanding.

The kinetic study showed a first-order rate dependency on the palladium and the substrate, whereas a zero-order dependency was observed for  $\text{PhI(TFA)}_2$  (Fig. 1).<sup>12</sup> The isotope labelling experiment showed a high value of kinetic isotope effect (KIE = 3.02) (Scheme 6). Such a high value of KIE unambiguously establishes C–H activation as the rate limiting step.



Scheme 4 Detection of acetate release.<sup>10</sup>





Scheme 5 Evidence in support of Pd–arene interaction.

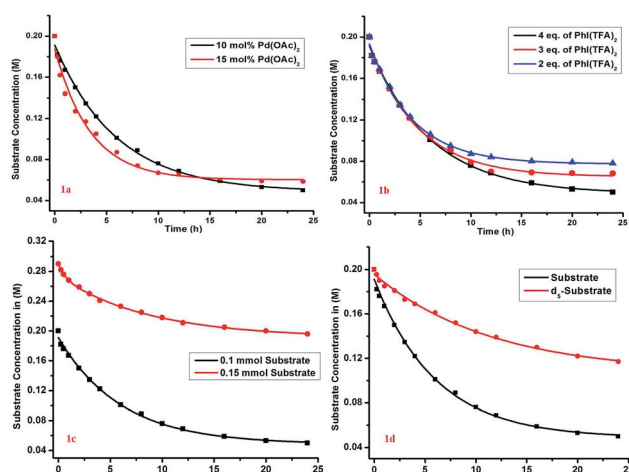
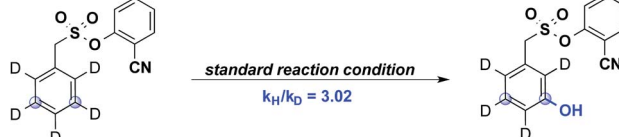


Fig. 1 Order determination: (a) overlay of reaction profile with 10 mol% and 15 mol% Pd; (b) reaction profiles with different  $\text{PhI}(\text{TFA})_2$  loadings. The reactions were performed with 0.1 mmol substrate, 10 mol% Pd, 25 mol% ligand and 0.5 mL of HFIP with variation in  $\text{PhI}(\text{TFA})_2$  only as 2 eq., 3 eq. and 4 eq. (c) order determination w.r.t. to substrate (order = 1). Reactions are done on a 0.1 and 0.15 mmol scale (d) determination of the kinetic isotope effect ( $k_{\text{H}}/k_{\text{D}} = 3.02$ ). Reactions are done with the model substrate and  $\text{d}_5$ -substrate on a 0.1 mmol scale. In (c) and (d) all the reactions are performed with 10 mol% catalyst, 25 mol% ligand, 4 equiv. of  $\text{PhI}(\text{OTFA})_2$  and 0.5 mL (0.1 mmol scale) of HFIP at 70 °C.

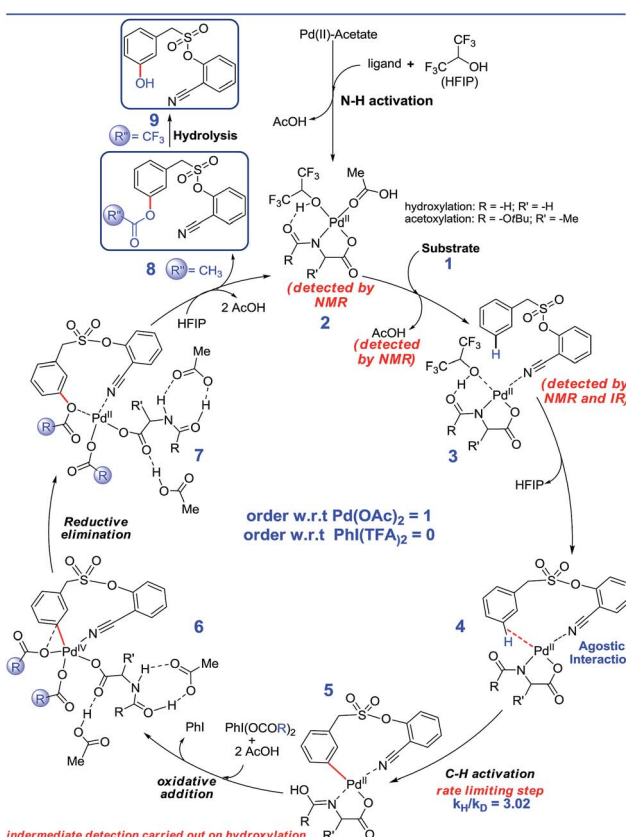
### DFT calculation

Guided by these experimental observations, we have also conducted density functional theory computations to arrive at a plausible mechanistic pathway (Scheme 7). It is worth mentioning that the *meta* selective olefination pathway has been computationally investigated jointly by the Yu, Wu and Houk groups to illustrate the role of the *N*-protected amino acid in remote C–H activation.<sup>15</sup> However, the *meta* selective C–O bond formation reaction is yet to be addressed using *in silico* studies. Contextually, DFT studies were carried out using the SMD/M06/

### Kinetic Isotope Effect



Scheme 6 Determination of the kinetic isotope effect.



Scheme 7 A plausible mechanism.

6–31G\*\* level of theory to locate key intermediates and transition states involved in the catalytic cycle.<sup>16</sup> Two ligands, namely For-Gly-OH and Boc-Ala-OH, were used in our computational study.

First, different likely active species were examined by varying the ligand combinations around the Pd(II). Deprotonation of the carboxyl and amino groups of the ligand by the Pd-bound acetates led to the formation of an amino acid chelated Pd(II) intermediate (**b**;<sup>17</sup> Fig. 2), and labile acetic acid ligands on the Pd center. Experimentally, HFIP was found to be vital for the title reaction. Hence the solvent HFIP was probed to study its potential influence on the energetics of the reaction. Notably, the HFIP binding, as in intermediate **2**, was 1.5 kcal mol<sup>−1</sup> lower than the corresponding acetic acid binding.<sup>18</sup> This prediction is in accordance with our NMR identification of intermediate **2**. The active species generated through the binding of the amino acid ligand to Pd(II) participated in the catalytic cycle as described below. The major mechanistic steps consist of (a)

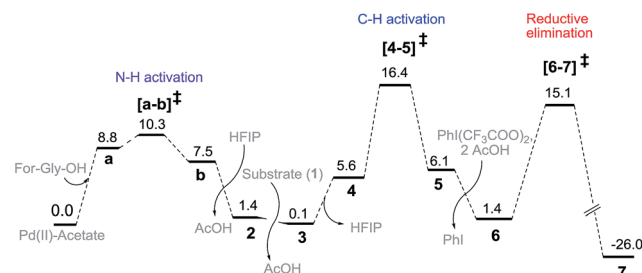
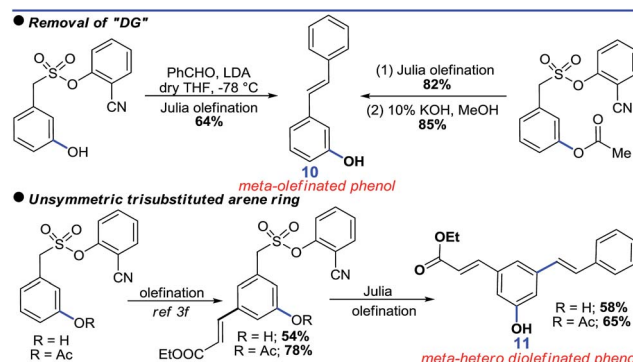


Fig. 2 Gibbs free energy profile ( $\text{kcal mol}^{-1}$ ) of the *meta* hydroxylation obtained at the SMD/M06/6-31G\*\*, LANL2DZ(Pd) level of theory.

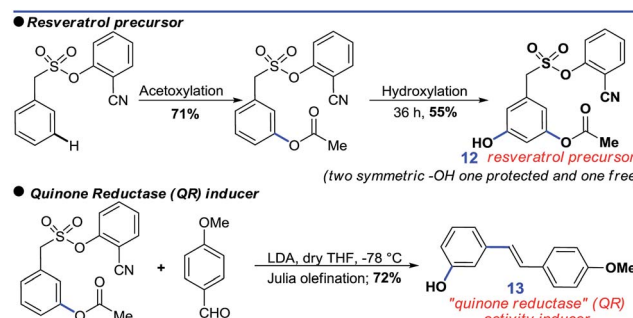
substrate uptake through ligand exchange, (b) ligand-assisted C–H activation, (c) oxidative addition to  $\text{PhI}(\text{OCOR})_2$ , and (d) reductive elimination leading to  $\text{C}_{\text{aryl}}\text{–O}$  bond formation (Scheme 7).

Substrate binding through the cyano group has been considered to direct palladium to the *meta*-C–H bond as in intermediate 3. Although intermediate 3 could have either neutral acetic acid or HFIP coordination, HFIP was found to be moderately preferred.<sup>19</sup> Among the various possibilities for ligand assisted C–H activation, the abstraction of the  $\text{C}_{\text{aryl}}\text{–H}$  proton by the amino acid ligand (Fig. 3) was found to be much more preferred (by 4.8 kcal mol<sup>–1</sup>) over the generally proposed acetate-assisted C–H activation.<sup>20</sup>

The palladated aryl thus formed underwent oxidative insertion to yield penta-coordinate Pd(IV) intermediate 6. In the following vital step, reductive elimination (RE) led to the formation of the  $\text{C}_{\text{aryl}}\text{–OCOR}$  bond ( $\text{R} = \text{CH}_3$  or  $\text{CF}_3$ ). In the most preferred RE transition state, mono-dentate binding of the amino acid ligand (Fig. 3) was found to be preferred over the chelated form.<sup>21</sup> At this stage of the reaction, the uptake of an HFIP molecule could assist the release of the product from the catalyst–product complex (7) to regenerate the active species (2).<sup>22</sup> A more interesting aspect at this juncture is the fate of the resulting acetylated or trifluoro-acetylated product. Experimental observation suggests that the trifluoroacetylated product is hydrolysed to yield a *meta*-hydroxylated compound whereas the acetylated product continues to remain as it is under identical reaction conditions. The origin of this kind of product distribution is traced to the lower



Scheme 8 Applicatory removal of the DG.



Scheme 9 Application of the protocol.

energy transition state for acid catalyzed hydrolysis in the case of the trifluoroacetate.<sup>23</sup>

## Application

Although the DG promoted *meta*-C–H functionalization, its removal will be crucial for the synthetic utility of such a strategy. In this context, both the acetylated and hydroxylated compounds formed hydroxyl-stilbenes *via* Julia olefination (10, Scheme 8). An unsymmetric trisubstituted phenol was also generated using a similar approach (11, Scheme 8).

Further sequential acetylation and hydroxylation resulted in the formation of a potential resveratrol precursor (12). A phase II “Quinone Reductase” (QR) activity inducer (13) has also been synthesized using the present protocol (Scheme 9).<sup>24</sup>

## Conclusions

In summary, we have developed the first template assisted palladium catalyzed direct *meta*-hydroxylation strategy, which was further extended to a *meta*-acetylation reaction. Interestingly, the variation of R ( $\text{R} = \text{H}, \text{F}$ ) on the acetylating agent  $\text{PhI}(\text{OCOR}_3)_2$  led to the formation of different target molecules under similar reaction conditions. Mechanistic studies revealed the interesting role of the HFIP in the catalytic cycle. The approach has also been utilized for the synthesis of unsymmetrically substituted phenols and a QR activity inducer to demonstrate the synthetic utility of the protocol.

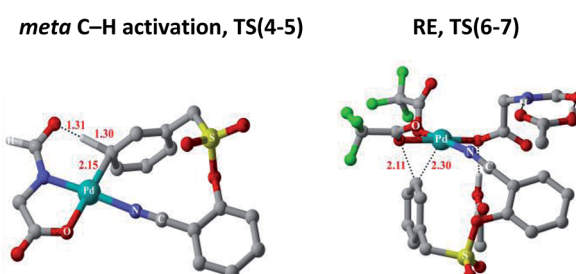


Fig. 3 Transition state geometries of two critical steps involved in the *meta*-hydroxylation. Selected hydrogen atoms shown only (distances are in Å).



## Acknowledgements

This activity is supported by SERB, India (EMR/2015/000164). Generous computing time from IIT Bombay supercomputing is acknowledged.

## Notes and references

- (a) J. Yamaguchi, A. D. Yamaguchi and K. Itami, *Angew. Chem., Int. Ed.*, 2012, **51**, 8960–9009; (b) T. Newhouse and P. S. Baran, *Angew. Chem., Int. Ed.*, 2011, **50**, 3362–3374; (c) R. Jazzar, J. Hitce, A. Renaudat, J. Sofack-Kreutzer and O. Baudoin, *Chem.-Eur. J.*, 2010, **16**, 2654–2672; (d) D. Y. K. Chen and S. W. Youn, *Chem.-Eur. J.*, 2012, **18**, 9452–9474; (e) S. D. Roughley and A. M. Jordan, *J. Med. Chem.*, 2011, **54**, 3451–3479; (f) J. Chao, H. Li, K. W. Cheng, M. S. Yu, R. C. Chang and M. Wang, *J. Nutr. Biochem.*, 2010, **21**, 482–489.
- (a) S. R. Neufeldt and M. S. Sanford, *Acc. Chem. Res.*, 2012, **45**, 936–946; (b) K. M. Engle, T. S. Mei, M. Wasa and J. Q. Yu, *Acc. Chem. Res.*, 2012, **45**, 788–802; (c) M. H. Holthausen, T. Mahdi, C. Schlepphorst, L. J. Hounjet, J. J. Weigand and D. W. Stephan, *Chem. Commun.*, 2014, **50**, 10038–10040; (d) G. Ménard and D. W. Stephan, *Angew. Chem., Int. Ed.*, 2012, **51**, 4409–4412; (e) G. Ménard, J. A. Hatnean, H. J. Cowley, A. J. Lough, J. M. Rawson and D. W. Stephan, *J. Am. Chem. Soc.*, 2013, **135**, 6446–6449; (f) M. Tobisu and N. Chatani, *Science*, 2014, **343**, 850–851; (g) L. T. Pilarski, N. Selander, D. Böse and K. J. Szabó, *Org. Lett.*, 2009, **11**, 5518–5521; (h) H. Grennberg and J. E. Bäckvall, *Chem.-Eur. J.*, 1998, **4**, 1083–1089.
- (a) D. Zhao, C. Nimpfius, M. Lindale and F. Glorius, *Org. Lett.*, 2013, **15**, 4504–4507; (b) G. D. Yu, T. Gensch, F. de Azambuja, S. Vásquez-Céspedes and F. Glorius, *J. Am. Chem. Soc.*, 2014, **136**, 17722–17725; (c) H. Wang, N. Schröder and F. Glorius, *Angew. Chem., Int. Ed.*, 2013, **52**, 5386–5389; (d) C. Grohmann, H. Wang and F. Glorius, *Org. Lett.*, 2013, **15**, 3014–3017; (e) P. Fang, M. Li and H. Ge, *J. Am. Chem. Soc.*, 2010, **132**, 11898–11899; (f) C. P. Ting and T. J. Maimone, *Angew. Chem., Int. Ed.*, 2014, **53**, 3115–3119; (g) N. Kuhl, M. N. Hopkinson, J. Wencel-Delord and F. Glorius, *Angew. Chem., Int. Ed.*, 2012, **51**, 10236–10254; (h) X. Chen, K. M. Engle, D. H. Wang and J. Q. Yu, *Angew. Chem., Int. Ed.*, 2009, **48**, 5094–5115; (i) S. R. Neufeldt and M. S. Sanford, *Acc. Chem. Res.*, 2012, **45**, 936–946; (j) M. S. Sigman and E. W. Werner, *Acc. Chem. Res.*, 2012, **45**, 874–884; (k) Y. Aihara and N. Chatani, *J. Am. Chem. Soc.*, 2013, **135**, 5308–5311; (l) G. Rouquet and N. Chatani, *Angew. Chem., Int. Ed.*, 2013, **52**, 11726–11743; (m) Z. Chen, B. Wang, Z. Wang, G. Zhu and J. Sun, *Angew. Chem., Int. Ed.*, 2013, **52**, 2027–2031; (n) W. Zhao, Z. Wang, B. Chu and J. Sun, *Angew. Chem., Int. Ed.*, 2015, **54**, 1910–1913.
- (a) T. W. Lyons and M. S. Sanford, *Chem. Rev.*, 2010, **110**, 1147–1169; (b) D. A. Colby, R. G. Bergman and J. A. Ellman, *Chem. Rev.*, 2010, **110**, 624–655.
- (a) J. Y. Cho, M. K. Tse, D. Holmes, R. E. Maleczka and M. R. Smith, *Science*, 2002, **295**, 305–308; (b) T. Ishiyama, J. Takagi, K. Ishida, N. Miyaura, N. R. Anastasi and J. F. Hartwig, *J. Am. Chem. Soc.*, 2002, **124**, 390–391; (c) R. J. Phipps and M. J. Gaunt, *Science*, 2009, **323**, 1593–1597; (d) O. Saidi, J. Marafie, A. E. W. Ledger, P. M. Liu, M. F. Mahon, G. Kociok-Köhn, M. K. Whittlesey and C. G. Frost, *J. Am. Chem. Soc.*, 2011, **133**, 19298–19301; (e) H. A. Duong, R. E. Gilligan, M. L. Cooke, R. J. Phipps and M. J. Gaunt, *Angew. Chem., Int. Ed.*, 2011, **50**, 463–466; (f) F. Juliá-Hernández, M. Simonetti and I. Larrosa, *Angew. Chem., Int. Ed.*, 2013, **52**, 11458–11460; (g) N. Hofmann and L. Ackermann, *J. Am. Chem. Soc.*, 2013, **135**, 5877–5884; (h) C. Cheng and J. F. Hartwig, *Science*, 2014, **343**, 853–857; (i) J. Schranck, A. Tlili and M. Beller, *Angew. Chem., Int. Ed.*, 2014, **53**, 9426–9428; (j) A. J. Martínez-Martínez, A. R. Kennedy, R. E. Mulvey and C. T. O'Hara, *Science*, 2014, **346**, 834–837.
- (a) J. Cornella, M. Righi and I. Larrosa, *Angew. Chem., Int. Ed.*, 2011, **50**, 9429–9432; (b) J. Luo, S. Preciado and I. Larrosa, *J. Am. Chem. Soc.*, 2014, **136**, 4109–4112; (c) J. Luo, S. Preciado and I. Larrosa, *Chem. Commun.*, 2015, **51**, 3127–3130; (d) J. Luo, S. Preciado, S. O. Araromi and I. Larrosa, *Chem.-Asian J.*, 2015, **6**, 5595–5600; (e) Y. Kuninobu, H. Ida, M. Nishi and M. Kanai, *Nat. Chem.*, 2015, **7**, 712–717; (f) X.-C. Wang, W. Gong, L. Z. Fang, R. Y. Zhu, S. Li, K. M. Engle and J.-Q. Yu, *Nature*, 2015, **519**, 334–338; (g) Z. Dong, J. Wang and G. Dong, *J. Am. Chem. Soc.*, 2015, **137**, 5887–5890; (h) P. X. Shen, X. C. Wang, P. Wang, R. Y. Zhu and J.-Q. Yu, *J. Am. Chem. Soc.*, 2015, **137**, 11574–11577.
- D. Leow, G. Li, T. S. Mei and J. Q. Yu, *Nature*, 2012, **486**, 518–522.
- (a) H. X. Dai, G. Li, X. G. Zhang, A. F. Stepan and J. Q. Yu, *J. Am. Chem. Soc.*, 2013, **135**, 7567–7571; (b) L. Wan, N. Dastbaravardeh, G. Li and J. Q. Yu, *J. Am. Chem. Soc.*, 2013, **135**, 18056–18059; (c) R. Y. Tang, G. Li and J. Q. Yu, *Nature*, 2014, **507**, 215–220; (d) G. Yang, P. Lindovska, D. Zhu, J. Kim, P. Wang, R. Y. Tang, M. Movassaghi and J. Q. Yu, *J. Am. Chem. Soc.*, 2014, **136**, 10807–10813; (e) Y. Deng and J. Q. Yu, *Angew. Chem., Int. Ed.*, 2015, **54**, 888–891.
- (a) S. Lee, H. Lee and K. L. Tan, *J. Am. Chem. Soc.*, 2013, **135**, 18778–18781; (b) M. Bera, A. Modak, T. Patra, A. Maji and D. Maiti, *Org. Lett.*, 2014, **16**, 5760–5763; (c) M. Bera, A. Maji, S. K. Sahoo and D. Maiti, *Angew. Chem., Int. Ed.*, 2015, **54**, 8515–8519; (d) S. Li, H. Ji, L. Cai and G. Li, *Chem. Sci.*, 2015, **6**, 5595–5600.
- (a) N. Itoh, T. Sakamoto, E. Miyazawa and Y. Kikugawa, *J. Org. Chem.*, 2002, **67**, 7424–7428; (b) R. M. Moriarty, *J. Org. Chem.*, 2005, **70**, 2893–2903; (c) V. S. Thirunavukkarasu, J. Hubrich and L. Ackermann, *Org. Lett.*, 2012, **14**, 4210–4213; (d) D. J. Gallardo and R. Martin, *J. Am. Chem. Soc.*, 2013, **135**, 9350–9353; (e) H. Y. Zhang, H. M. Yi, G. W. Wang, B. Yang and S. D. Yang, *Org. Lett.*, 2013, **15**, 6186–6189; (f) F. Yang and L. Ackermann, *Org. Lett.*, 2013, **15**, 718–720; (g) Y. M. Xing, L. Zhang and D. C. Fang,



*Organometallics*, 2015, **34**, 770–777; (h) C. Cheng, S. Liu and G. Zhu, *J. Org. Chem.*, 2015, **80**, 7604–7612; (i) Q. R. Liu, C. X. Pan, X. P. Ma, D. L. Mo and G. F. Su, *J. Org. Chem.*, 2015, **80**, 6496–6501; (j) C. Yang, X. G. Zhang, D. Zhang-Negrerie, Y. Du and K. Zhao, *J. Org. Chem.*, 2015, **80**, 5320–5328; (k) T. Zhou, F. X. Luo, M. Y. Yang and Z. J. Shi, *J. Am. Chem. Soc.*, 2015, **137**, 14586–14589; (l) S. Z. Sun, M. Shang, H. L. Wang, H. X. Lin, H. X. Dai and J. Q. Yu, *J. Org. Chem.*, 2015, **80**, 8843–8848; (m) Y. H. Zhang and J. Q. Yu, *J. Am. Chem. Soc.*, 2009, **131**, 14654–14655.

11 (a) P. Y. Choy and F. Y. Kwong, *Org. Lett.*, 2013, **15**, 270–273; (b) G. Shan, X. Yang, L. Ma and Y. Rao, *Angew. Chem., Int. Ed.*, 2012, **51**, 13070–13074.

12 See ESI† for more details.

13 Details of CCDC 1417521 (1l), 1417522 (2o), and 1417523 (2q) are available via [www.ccdc.cam.ac.uk/data\\_request/cif](http://www.ccdc.cam.ac.uk/data_request/cif).

14 U. Sharma, T. Naveen, A. Maji, S. Manna and D. Maiti, *Angew. Chem., Int. Ed.*, 2013, **52**, 12669–12673.

15 (a) G. J. Cheng, Y. F. Yang, P. Liu, P. Chen, T. Y. Sun, G. Li, X. G. Zhang, K. N. Houk, J. Q. Yu and Y. D. Wu, *J. Am. Chem. Soc.*, 2014, **136**, 894–897; (b) Y. F. Yang, G. J. Cheng, P. Liu, D. Leow, T. Y. Sun, P. Chen, X. G. Zhang, J. Q. Yu, Y. D. Wu and K. N. Houk, *J. Am. Chem. Soc.*, 2014, **136**, 344–355.

16 M. J. Frisch *et. al.* (a) Full details of the computational methods are provided in the ESI.†; (b) Gaussian09 quantum chemical suite has been used for the computations

17 (a) G.-J. Cheng, Y.-F. Yang, P. Liu, D. Leow, T. Y. Sun, P. Chen, X. Zhang, J. Q. Yu, Y. D. Wu and K. N. Houk, *J. Am. Chem. Soc.*, 2014, **136**, 894; (b) More details in ESI Fig. S4 and S9.†

18 The replacement of both acetic acid ligands by two HFIP molecules is energetically higher than substitution of just one HFIP (See Fig. S5 and S10 in the ESI†).

19 Link to the results and relative energies of intermediates in the ESI. [Fig. S6 and S11†].

20 (a) We have also compared the *ortho* as well as *para* C–H activation to learn that the *meta* is energetically most preferred. See Tables S20, 21, Fig. S7 and S12 in the ESI.†; (b) D. G. Musaev, A. Kaledin, B.-F. Shi and J. Q. Yu, *J. Am. Chem. Soc.*, 2011, **134**, 1690

21 (a) More details of the RE possibilities are provided in Fig. S8 and S13 in the ESI.† For examples of RE for a penta coordinated Pd(IV) see; (b) D. M. Crumpton and K. I. Goldberg, *J. Am. Chem. Soc.*, 2000, **122**, 962; (c) A. R. Dick, J. W. Kampf and M. S. Sanford, *J. Am. Chem. Soc.*, 2005, **127**, 12790.

22 More details are provided in the ESI (See Fig. S7, S8 and Table S20†).

23 (a) More details are provided in Fig. S15 in the ESI.†; (b) R. Gómez-Bombarelli, E. Calle and J. Casado, *J. Org. Chem.*, 2013, **78**, 6880

24 W. Zhang and M. L. Go, *Eur. J. Med. Chem.*, 2007, **42**, 841–850.

